

## Catalytic partial oxidation of methane to synthesis gas in a ceramic membrane reactor

A. Santos, J. Coronas, M. Menéndez and J. Santamaría

*Department of Chemical and Environmental Engineering, University of Zaragoza,  
50009 Zaragoza, Spain*

Received 21 July 1994; accepted 11 October 1994

Methane has been selectively converted to synthesis gas using a two-zone fixed bed of a Ni/Al<sub>2</sub>O<sub>3</sub> catalyst inside a modified ceramic membrane. The first zone of the reactor was surrounded by an impervious wall, and therefore behaved as a conventional fixed bed reactor. In the second zone, some of the reaction products could preferentially diffuse out of the reactor, which yielded higher than equilibrium methane conversions. The influence of the different operating conditions has been studied, and the performance of the membrane reactor has been compared to that of a fixed bed reactor. The membrane reactor has also been used at pressures above atmospheric (2 bar), with good conversions and selectivities.

**Keywords:** methane oxidation; synthesis gas; membrane reactors

### 1. Introduction

Natural gas is an increasingly important raw material in the chemical industry. Among other applications, methane is used as a starting material for the production of methanol and higher alcohols, ammonia, aldehydes and higher hydrocarbons. Synthesis gas plays an important role as an intermediate in all of the above processes, with different CO/H<sub>2</sub> ratios depending on the desired final product. The major routes for the production of synthesis gas from methane are steam reforming and autothermal reforming. The latter, which is a technology developed four decades ago, combines partial oxidation and adiabatic steam reforming, and has the advantage of avoiding the external heat input required in the steam reforming process. When the partial oxidation step is carried out without a catalyst, very high temperatures (1200–1500°C) are necessary in the burner to achieve high methane and oxygen conversions [1]. In addition, the catalytic reformer that follows the combustion chamber is exposed to the hot exit gases. At the exit of the reformer, the synthesis gas is approximately at the equilibrium composition given by the steam reforming and shift reactions.

With an appropriate catalyst in a partial oxidation reactor, the same exit compo-

sition can be obtained using a single unit instead of using the burner plus the reformer reactors. In addition, temperatures in the vicinity of 800°C are sufficient to achieve methane conversions higher than 90%. This process has been carried out using fixed bed reactors (e.g. refs. [2–4]), fluidized bed reactors [5,6] and monolith reactors [7,8].

Although there is experimental evidence [9,10] suggesting that, under certain conditions (e.g., temperatures higher than 1000°C, very short contact times and Pt or Rh catalysts), the catalytic partial oxidation of methane to synthesis gas may take place directly under different conditions (e.g., temperatures around 800°C and Ni-based catalysts), it seems that the process involves a combustion of part of the methane to CO and CO<sub>2</sub> followed by water–gas shift and steam and CO<sub>2</sub> reforming of the remaining methane [4,11].

Given sufficient contact time and temperature, several noble-metal and transition-metal catalysts have been found to give methane conversions and CO and H<sub>2</sub> selectivities close to equilibrium values (e.g., refs. [2,3,4,12]). Although equilibrium conversions at atmospheric pressure and temperatures around 800°C are rather high, the economics of the industrial process require operation at pressures of 20 bar and higher [1], which means that the equilibrium values are lowered considerably. Thus, for instance, at 825°C and atmospheric pressure the equilibrium conversion for a 2/1/1 CH<sub>4</sub>/O<sub>2</sub>/N<sub>2</sub> ratio is close to 95%, whereas at 20 bar the equilibrium value drops to around 63%.

In view of the above, a way to overcome equilibrium limitations must be found, in order to apply the catalytic partial oxidation of methane to syngas under the usual industrial conditions. Membrane reactors can provide such an opportunity, by allowing one or more of the reaction products to permeate out of the reactor, thus displacing equilibrium towards higher conversions. When, as in the present case, hydrogen is one of the reaction products, there are several possibilities for its removal from the reaction medium. In the past, dense metallic membranes have been used (usually made from Pd or Pd alloys), which are able to incorporate large amounts of hydrogen and enable the gas to diffuse away by virtue of the selective interaction of palladium and hydrogen. The field of palladium-based membrane reactors has been reviewed recently [13]. In spite of the relatively numerous laboratory applications, dense palladium membranes are costly, provide low fluxes, and suffer from metal sintering and fatigue, all of which restrict their industrial application.

A second possibility consists of supporting Pd on a porous medium, either as a thin film or as an impregnated phase. In the first case, the goal is to retain the hydrogen permselectivity provided by the Pd, while in the second, the metal fulfils the role of an active catalyst within a porous support. Examples of the first approach are the works of Gobina and Hughes [14], who applied an ion-sputtering technique to deposit a Pd–Ag thin layer on porous Vycor glass, and used it for ethane dehydrogenation, and of Kikuchi et al. [15,16], who used electroless plating to obtain a composite Pd–glass membrane in which to carry out the water–gas shift reaction.

The second process takes advantage of the porous nature of the membranes to introduce an active phase, often using standard impregnation techniques. Thus for instance, Sun and Khang [17] used a Pt-impregnated porous glass membrane for cyclohexane dehydrogenation, and Champagnie et al. [18] used Pt deposited on a porous alumina membrane to effect ethane dehydrogenation. Other applications can be found in the reviews by Hsieh [19] and by Saracco and Specchia [20].

Finally, hydrogen can also be removed from the reaction medium by using membranes with an appropriate pore distribution, which are only partially permselective. This is the case of numerous works on dehydrogenation reactions that have used porous membranes operating in the Knudsen region (e.g., refs. [21–25]). A very interesting configuration to carry out steam reforming at an industrial scale has been proposed by Adris et al. [26]. In this case the removal of hydrogen would be achieved by means of a membrane (either a palladium membrane or a ceramic membrane with narrow pores), immersed in the fluidized bed reactor used for the process. In spite of their lower selectivity towards permeation, porous ceramic membranes are attractive for industrial operation because they offer much higher fluxes than dense metallic membranes, at a fraction of the cost.

In this work, a membrane operating in the Knudsen diffusion regime has been used for the partial oxidation of methane to synthesis gas. Given the high temperatures involved (800°C and above), the usual commercial ceramic membranes are in general not immediately suitable for this reaction. Therefore, in this case, a modified ceramic membrane has been employed, which was originally developed for application in the methane oxidative coupling process [27,28].

## 2. Experimental

### 2.1. REACTOR CONCEPT

Fig. 1 shows a diagram of the reactor used. It consists of a conventional fixed bed reactor followed by a membrane reactor, both integrated in the same unit. The reactor wall is a commercial alumina membrane (SCT), whose pore distribution was modified as described below. The membrane had an internal diameter of 6.6 mm, and an outside diameter of 10 mm, with a total length of 375 mm. The separation layer had a nominal pore size of 200 nm. The membrane was housed within an external stainless steel shell, and the ensemble was heated by means of a two-zone furnace. Gas tightness between the membrane and the stainless steel shell was achieved using several 3 mm thick graphite rings, compressed in a flat-conical packing joint, which was especially designed to minimize the exposure of the graphite to the hot gases on the shell side.

On the tube side, a 14 cm long fixed bed containing approximately 3.5 g of NiO/NiAl<sub>2</sub>O<sub>4</sub> catalyst was packed in the annular space between the inner tube wall and an axial quartz thermowell, with an outside diameter of 4 mm. A movable thermocouple was inserted in the axial thermowell in order to measure the tempera-

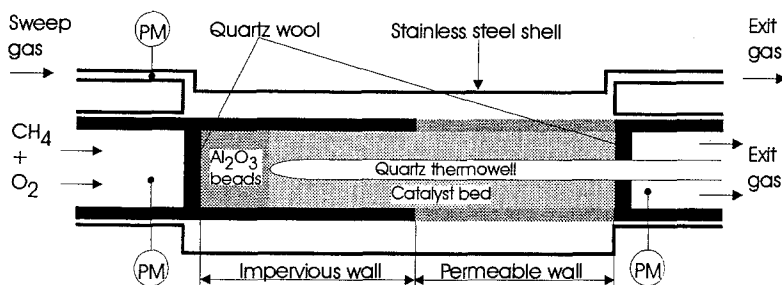


Fig. 1. Scheme of the reactor configuration.

tures along the catalyst bed as closely as possible. This is important in view of the possibility of undetected hot spots in the bed [29]. Preceding the catalyst, a 5 cm long bed of alpha-alumina beads (0.5–0.8 mm), served as a gas preheater.

The first 6 cm of the catalyst bed had an impervious wall. This was necessary in order to achieve a high enough concentration of reaction products previous to any permeation process. Otherwise, if the whole length of the catalyst bed was permeable, methane and oxygen would significantly permeate to the shell side in the entrance region of the bed. Therefore, the first part of the bed behaved as a conventional fixed bed reactor, in which a fast reaction occurred, producing synthesis gas under approximately equilibrium conditions. The gas stream then entered the next 8 cm of the bed, corresponding to the porous wall section, where preferential permeation of hydrogen took place, thereby driving equilibrium in the direction of higher methane conversions. In this system, different permeation flows can be achieved by varying the pressure gradient between the tube side and the shell side, as well as the flowrate of the sweep gas ( $N_2$ ) on the shell side. Otherwise, the reactor can be operated approximately as a conventional fixed bed reactor by closing the valves that control the flow on the shell side and waiting for a steady state to be achieved.

## 2.2. EXPERIMENTAL DETAILS

The permeability of the starting ceramic membrane was reduced by depositing silica inside its pores. To this end, a commercial silica sol (Akzo Chemie 40-AS) was used. The membrane was subjected to three cycles consisting of immersion in the silica sol for 1 h, drying at 130°C and calcination for 2 h at 800°C. After the three cycles, the membrane was further calcined for 72 h at 800°C. The impervious zones of the membrane were created by applying several layers of an enamel coating in the selected areas. Thus, of the 19 cm long reactor (preheating section + catalyst bed), only 8 cm (about 42%) were permeable.

The  $NiO/NiAl_2O_4$  catalyst, with a Ni concentration of approximately 10% by weight was prepared following the method used by Al-Ubaid and Wolf [30], with

some minor variations. The resulting solid was dried, calcined and sieved to a size between 250 and 500  $\mu\text{m}$ .

The partial oxidation of methane to syngas usually proceeds with considerable temperature gradients inside the reactor (e.g. ref. [4]). In this case, the temperature was kept constant at two points in the reactor axis, by means of the two-zone furnace, and the temperature profile along the bed was measured by a movable thermocouple. The two temperature control points were usually located 12 cm apart, the first one 2 cm inside the catalyst bed, and the second at the end of the catalyst bed. However, some experiments have been run with the control points at the two ends of the catalyst bed (i.e., 14 cm apart), in order to compare the resulting temperature profiles. Hereinafter, when reporting the results obtained, the temperature used will be the set point temperature, which is achieved at the two control points.

As indicated in fig. 1, the pressure is measured on the shell side, and before and after the catalyst bed on the tube side. Unless otherwise indicated, the pressures reported in this work correspond to the readings of the pressure transducer located at the beginning of the fixed bed. The outer stainless steel shell surrounding the membrane reactor was designed to be capable to withstand the pressure generated in the event of an accidental explosion of the reacting mixture. In addition, the pressure transducer at the beginning of the fixed bed was interlocked to a shutoff valve in order to interrupt the flow of reactants in case of a membrane rupture.

All the experiments presented in this work have been run with a mass-flow controlled feed mixture on the tube side containing  $\text{CH}_4$ ,  $\text{O}_2$  and  $\text{N}_2$  in a 2/1/1 ratio respectively, and pure  $\text{N}_2$  as the sweep gas on the shell side. The exit flowrates on the tube side and on the shell side were measured separately, and their compositions determined by gas chromatography. The mass balance closures were within  $\pm 3\%$  in all the experiments reported in this work.

The amount of carbon deposited on the catalyst after a given experiment was determined by burning off the carbonaceous deposits with  $\text{O}_2/\text{N}_2$  mixtures. All the gases produced in the combustion were then collected and analyzed for CO and  $\text{CO}_2$ , from which the total amount of carbon in the reactor could be determined.

The conversion of methane was calculated as 1 minus the ratio of the total number of moles of methane in both exit streams to the number of moles of methane in the feed. The selectivity towards CO was calculated as the number of moles of CO in both product streams divided by the number of moles of methane reacted, and the selectivity towards hydrogen as one half of the total number of moles of hydrogen in both product streams divided by the number of moles of methane reacted.

### 3. Results and discussion

As mentioned above, considerable temperature variations may take place in fixed bed reactors during the partial oxidation of methane. Fig. 2 shows two exam-

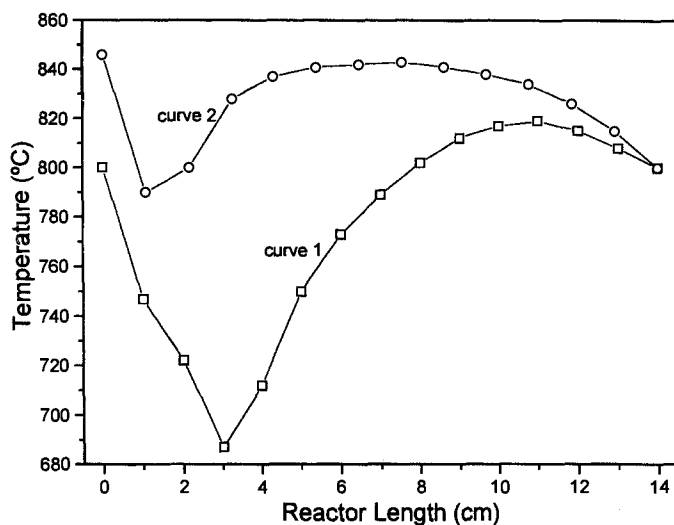


Fig. 2. Temperature profiles in the reactor with a temperature set point of 800°C. Curve 1: total flow rate = 100 cm<sup>3</sup>(STP)/min, temperature control points at  $x = 0$  and at  $x = 14$  cm. Curve 2: total flow rate = 175 cm<sup>3</sup>(STP)/min, temperature control points at  $x = 2$  and at  $x = 14$  cm.

ples of these, corresponding to experiments run without permeation to the shell side (i.e. conventional fixed bed reactor experiments). In both cases, the set point temperature is imposed at two control points in the reactor. Curve 1 shows the results obtained when the control points are located on both ends of the catalyst bed, with a temperature setpoint of 800°C. In this case, the resulting temperature profile shows a decrease of more than 110°C in the first 3 cm of the bed. When the first control thermocouple was moved 2 cm inside the catalyst bed while keeping the same setpoint value (curve 2), a large temperature increase occurs at the bed entrance, followed by a sharp decline in the first cm of the catalyst bed, and then a recovery, as the first temperature control point is approached. The results in both cases of fig. 2 agree with the picture of a fast combustion of part of the methane at the entrance of the bed, which would consume practically all the oxygen feed, followed by the endothermic steam and CO<sub>2</sub> reforming reactions of the unconverted methane. The temperature increases observed from 3 to 11 cm in curve 1 and from 2 to 7 cm in curve 2 are a consequence of the heat supplied by the two-zone furnace in order to meet the 800°C required at the second temperature control point.

The temperature profiles in the reactor are obviously important in the determination of the equilibrium conversions. Fig. 3 shows the calculated equilibrium values as a function of temperature, at three different pressures. The calculations were made using the calculation routines in PRO-II<sup>TM</sup> simulation software, assuming that no carbon is formed in the system. Given the important temperature variations in the bed, a significant shift in the equilibrium composition can be expected along the reactor. Thus, at atmospheric pressure and 800°C (temperature setpoint),

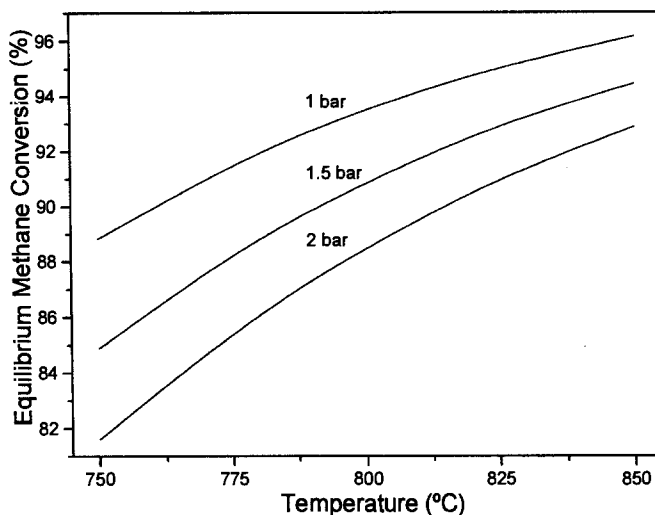


Fig. 3. Equilibrium conversion of methane at different temperatures and pressures.  $\text{CH}_4/\text{O}_2/\text{N}_2 = 2/1/1$ .

the equilibrium methane conversion is about 2.5 percentage points lower than at  $843^\circ\text{C}$  (the temperature maximum in curve 2 of fig. 2).

Fig. 4 shows the results obtained operating under conventional fixed bed reactor conditions, at approximately atmospheric pressure. The performance of the reactor, as measured by the conversions and selectivities at the reactor exit, was generally stable. After the experiments, the total amount of coke deposited on the

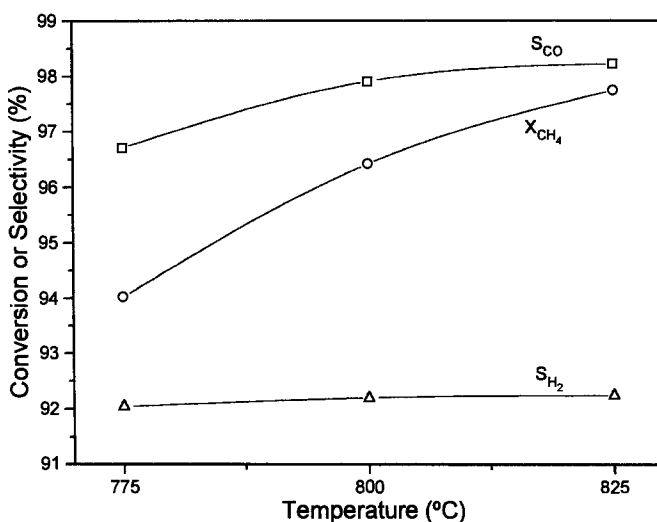


Fig. 4. Methane conversion and CO and  $\text{H}_2$  selectivities obtained in fixed bed reactor operation at three different temperatures. Total flow rate:  $100 \text{ cm}^3(\text{STP})/\text{min}$ , average pressure in the reactor: 1.1 bar.

catalyst could be measured by combustion of the coke deposits. The maximum levels of coke deposition were around 1.5% by weight, after 30 h of operation at 800°C. The results in fig. 4 show that the methane conversion and the CO selectivity clearly increase with temperature, while the increase in the selectivity to hydrogen is less marked. The quantitative data in fig. 4 can be explained by taking into account the temperature profiles in the bed. Thus for instance, if we take the methane conversion obtained at 800°C (96.4%), it is above the equilibrium value for this temperature (93.5%), but it is approximately the same as the equilibrium value at the temperature of the maximum (approximately 96%).

The effect of permeation through the membrane wall is shown in figs. 5a and 5b for setpoint temperatures of 800 and of 775°C, respectively. In this case, the advantages of permeation through the membrane wall have been investigated using nitrogen as the sweep gas on the shell side. However, in industrial operation steam would likely be used as the sweep gas instead of nitrogen, due to the fact that it can be separated more easily from the reaction products. Also, steam is part of the reaction atmosphere, and any steam permeating from the shell side to the tube

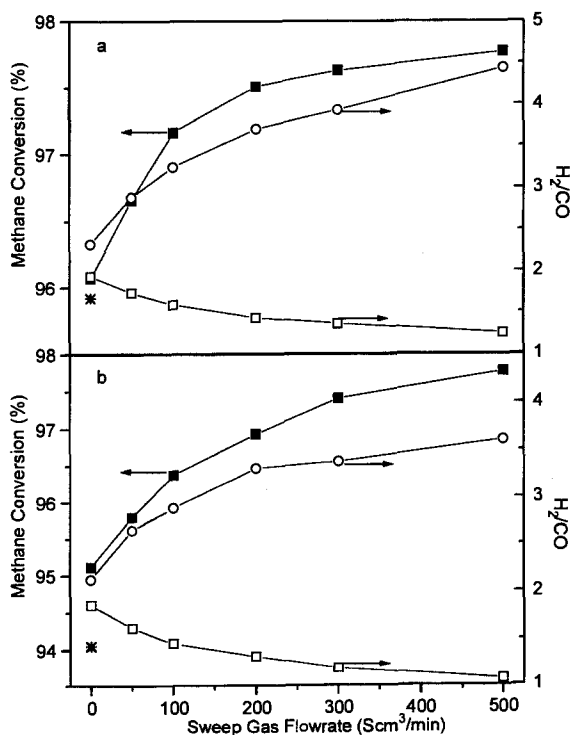


Fig. 5. Methane conversion and H<sub>2</sub>/CO ratio versus sweep gas flow rate. (a) Temperature: 800°C. (b) Temperature: 775°C. (a) and (b): Pressure: 1.13 bar, inlet flow rate (tube side): 175 cm<sup>3</sup>(STP)/min. (■) Total methane conversion. (\*) Total methane conversion without flow on the shell side (exit valve closed on the shell side). (□) H<sub>2</sub>/CO ratio at the exit of the tube side. (○) H<sub>2</sub>/CO ratio at the exit of the shell side.

side would contribute to the steam reforming and shift reactions already taking place in the catalyst bed.

The results in fig. 5 show that, as the sweep gas flowrate is increased, the methane conversion increases significantly, from the value corresponding to fixed bed reactor operation, denoted by an asterisk in the figure. Although the increase shown in these figures is of only a few percentage points, it is remarkable because it takes place over an initial value of methane conversion which is already very high. The effect of a higher sweep gas flowrate is to increase the differences in the partial pressures between the tube side and the shell side for the species present in the reactor. Since the type of membrane used in this work is expected to provide permeation fluxes which are approximately in the Knudsen regime [27], the diffusion of hydrogen (a reaction product) should take place preferentially, thereby shifting the equilibrium towards higher conversions, as shown in figs. 5a and 5b. The preferential permeation of hydrogen is also demonstrated in these figures by the curves showing a considerably higher  $H_2/CO$  ratio at the exit of the shell side, compared to the tube side.

An interesting feature of the results presented in figs. 5a and 5b is that the conversion values corresponding to zero sweep gas flowrate are higher than those corresponding to conventional fixed bed operation. This means that, even in the absence of sweep gas, permeation was taking place, and a small exit flow ( $54 \text{ cm}^3(\text{STP})/\text{min}$  in this case), could be measured on the shell side under the conditions indicated. When the flow of the sweep gas was established, the permeation allowed high conversions to be obtained even under relatively high flowrates. Thus for instance, with a sweep gas flowrate of  $500 \text{ cm}^3(\text{STP})/\text{min}$ , conversions of 94.4% could still be obtained when the inlet flow rate on the tube side was increased to  $500 \text{ cm}^3/\text{min}$ .

As mentioned above, under industrial conditions the partial oxidation of methane to syngas is carried out at relatively high pressures, which decrease the equilibrium conversions attained. Although the laboratory reactor used in this work was not designed to work at elevated pressures, some experiments have been run with pressures above 1 atm, in order to ascertain the usefulness of a membrane reactor to overcome the disadvantages of the operation at higher pressures.

Figs. 6a and 6b show the comparison of the results of methane conversion and  $H_2$  and CO selectivities at two different operating pressures. As expected, the use of a higher pressure considerably lowers the conversions obtained because of the unfavourable equilibrium conditions. However, in the membrane reactor the difference can be compensated by increasing the removal of reaction products through the membrane wall. Thus, at high values of the sweep gas flowrate the conversion of methane at 2 bar approaches that obtained in the atmospheric pressure reactor. As for the product selectivities, the selectivity to hydrogen increases with the sweep gas flowrate as it is preferentially removed by permeation, while the selectivity to CO, with a higher molecular weight remains at an approximately constant value.

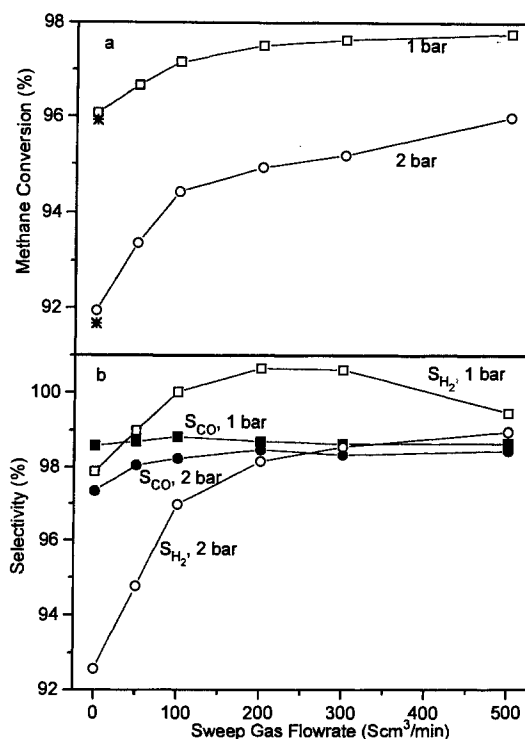


Fig. 6. Methane conversion (a) and  $\text{H}_2/\text{CO}$  selectivities (b) versus sweep gas flow rate, at  $800^\circ\text{C}$  and two different pressures.

#### 4. Conclusions

The reactor developed in this work, consisting of a fixed bed reactor followed by a ceramic membrane reactor, can give high yields for the partial oxidation of methane to synthesis gas. The diffusion of part of the reacting mixture through the membrane wall takes place approximately in the Knudsen regime. Therefore, hydrogen permeates preferentially and, as a consequence, higher than equilibrium conversions can be achieved.

At higher pressures, a decrease in the methane conversion takes place, due to the unfavourable equilibrium shift. However, the use of the membrane reactor allowed an increase of conversion which compensated the lower equilibrium values. This opens up a potential field of application of membrane reactors for the catalytic partial oxidation of methane to synthesis gas.

#### Acknowledgement

This work was carried out with financial support from DGA (P-IT-4/91) and DGICYT (PB90-0920 and PB93-0311).

## References

- [1] T.S. Christensen and I.I. Primdahl, *Hydroc. Process.* 73 (1994) 39.
- [2] A.T. Ashcroft, A.K. Cheetham, J.S. Foord, M.L.H. Green, C.P. Grey, A.J. Murrell and P.D.F. Vernon, *Nature* 344 (1990) 319.
- [3] D. Dissanayake, P. Rosynek, K.C.C. Kharas and J.H. Lunsford, *J. Catalysis* 132 (1991) 117.
- [4] W.J.M. Vermeiren, E. Blomsma and P.A. Jacobs, *Catal. Today* 13 (1992) 427.
- [5] S.S. Bharadwaj and L.D. Schmidt, *J. Catal.* 146 (1994) 11.
- [6] A. Santos, M. Menéndez and J. Santamaría, *Catal. Today*, accepted.
- [7] J.K. Hochmuth, *Appl. Catal. B* 1 (1992) 89.
- [8] P.M. Torniainen, X. Chu and L.D. Schmidt, *J. Catal.* 146 (1994) 1.
- [9] D.A. Hickman and L.D. Schmidt, *J. Catal.* 138 (1992) 267.
- [10] D.A. Hickman and L.D. Schmidt, *Science* 259 (1993) 343.
- [11] F. van Looij, J.C. van Giezen, E. Dorrestijn and J.W. Geus, *Proc. 4th Eur. Workshop on Methane Activation*, Eindhoven 1994.
- [12] P.D.F. Vernon, M.L.H. Green, A.K. Cheetham and A.T. Ashcroft, *Catal. Today* 13 (1992) 417.
- [13] J. Shu, B.P.A. Grandjean, A. Van Neste and S. Kaliaguine, *Can. J. Chem. Engin.* 69 (1991) 1036.
- [14] E. Gobina and R. Hughes, *J. Membr. Sci.* 90 (1994) 11.
- [15] E. Kikuchi, S. Uemiya, N. Sato, H. Inoue, H. Ando and T. Matsuda, *Chem. Lett.* (1989) 489.
- [16] S. Uemiya, N. Sato, H. Ando and E. Kikuchi, *Ind. Eng. Chem. Res.* 20 (1991) 589.
- [17] Y.M. Sun and S.J. Khang, *Ind. Eng. Chem. Res.* 27 (1988) 1136.
- [18] A.M. Champagnie, T.T. Tsotsis, R.G. Minet and E.G. Wagner, *J. Catal.* 134 (1992) 713.
- [19] H.P. Hsieh, *Catal. Rev.-Sci. Eng.* 33 (1991) 1.
- [20] G. Saracco and V. Specchia, *Catal. Rev. Sci. Eng.* 36 (1994) 305.
- [21] O. Shinji, M. Misono and Y. Yoneda, *Bull. Chem. Soc. Jpn.* 55 (1982) 2760.
- [22] T. Okubo, K. Haruta, K. Kusakabe, S. Morooka, H. Anzai and S. Akiyama, *Ind. Eng. Chem. Res.* 30 (1991) 614.
- [23] Z.D. Ziaka, R.G. Minet and T.T. Tsotsis, *AIChE J.* 39 (1993) 526.
- [24] F. Tiscareno-Lechuga, C.G. Hill and M.A. Anderson, *Appl. Catal. A* 96 (1993) 33.
- [25] T.T. Tsotsis, A.M. Champagnie, S.P. Vasileiadis, Z.D. Ziaka and R.G. Minet, *Chem. Eng. Sci.* 47 (1992) 2903.
- [26] A.M. Adris, S.S.E.H. Elnashaie and R. Hughes, *Can. J. Chem. Engin.* 69 (1991) 1061.
- [27] D. Lafarga, J. Santamaría and M. Menéndez, *Chem. Engin. Sci.* 49 (1994) 2005.
- [28] J. Coronas, M. Menéndez and J. Santamaría, *Chem. Engin. Sci.* 49 (1994) 2015.
- [29] D. Dissanayake, M.P. Rosynek and J.H. Lunsford, *J. Phys. Chem.* 97 (1993) 3644.
- [30] A. Al-Ubaid and E.E. Wolf, *Appl. Catal.* 40 (1988) 73.